Design and Implementation of Welding Mobile Robot Using a Proposed Control Scheme Based On Its Developed Dynamic Modeling for Tracking Desired Welding Trajectory

Nguyen Hung, Ho Dac Loc

HUTECH Institute of Engineering, HUTECH University of Technology, Vietnam

Abstract—This paper presents a proposed control scheme that makes the combination of a kinematic controller (KC) and an integral sliding mode controller (ISMC) for a welding mobile robot (WMR) to track a desired welding path. First, a posture tracking error vector is defined and a kinematic controller is designed based on kinematic modeling to make the tracking error vector go to zero asymptotically. Second, a sliding surface vector is defined based on the velocity tracking error vector and its integral term. And then, an integral sliding mode dynamic controller is designed based on developed dynamic modeling to make velocity tracking error vector also go to zero asymptotically. The above controllers are obtained by backstepping method. The stability of system is proved based on the Lyapunov stability theory. To implement the designed tracking controller, a control system is developed based on DSP F28355 and ATmega328. A scheme for measuring the posture tracking error vector using torch sensor is presented. The simulation and experiment results are shown to illustrate effectiveness and the applicability to the welding industry field of the proposed controller.

Keywords—Kinematic Controller (KC), Integral Sliding Mode controller (ISMC), Welding mobile robot (WMR), Lyapunov Stability Therory.

I.   INTRODUCTION

Over the past few decades, the sliding mode control (SMC) technique for nonlinear mechanical systems has been studied extensively by many researchers [1-15]. The main idea of using the SMC approach is to cope with the parametric uncertainties and external disturbances under matching conditions for the complex nonlinear systems exist in practical applications such as robotics manipulator, welding mobile robot,...[1,2]. Recently, many robust control algorithms using SMC [8-15] or combined with fuzzy logic [7], neural network [4,6], adaptive [3-4] have been proposed to deal with the trajectory tracking problem including system dynamics

[3-15]. Most of them, they used a control scheme of integrating a kinematic modeling into a dynamic modeling [4-7,9-14] or used only kinematic controller [8]. However, the linear velocity of mobile robot [9-12] or welding point of welding mobile robot was not keep constant velocity smoothly as desired [13-14]. Hung, et al. [15] proposes a new tracking controller that combines a kinematic controller and an integral sliding mode dynamic controller for an omnidirectional mobile platform to track a desired trajectory at a desired velocity of an OMP under disturbance and surface friction. It guarantees that the mobile robot has a good traking performance.

To solve the problem of trajectory tracking of welding mobile robot, this research presents a proposed control scheme that makes the combination of a kinematic controller (KC) based on the kinematic modeling and an integral sliding mode dynamic controller (ISMC) based on the developed dynamic modeling considering at voltage level for the WMR to track a desired welding trajectory at a desired velocity. The above controllers are obtained by backstepping method. The system stability is proved using the Lyapunov stability theory. To implement the designed tracking controller, a control system is developed based on DSP F28355 and ATmega328. A scheme for measuring the posture tracking error vector using torch sensor is presented. The simulation and experiment results are shown to illustrate effectiveness of the proposed nonlinear controller.

II.   SYSTEM DESCRIPTION AND MODELING

In this section, the system description, dc servo motor modeling, the kinematic and dynamic models of a welding mobile robot (WMR) are presented.

1.   System description

Fig. 1 shows the 3D configuration of a welding mobile robot (WMR) used in this research in three sides. It consists of platform, two wheels, DC servo motors and encoders, welding torch, power supply and a electronic

control system, etc. Fig. 2 shows the 2D configuration for geometric model of the WMR. For simplifying the modeling of WMR, the assumptions are given as follows [10-14]:

(1) Kinematic's parameters such as wheel's radius r and distance b are known exactly.

(2) Moment of inertia of WMR is constant during welding process.

(3) A disturbance vector exerted on the WMR consists of surface friction and slip phenomenon bewteen wheel and the ground.

(4) Motion surface is a smooth horizontal plane.

(5) The WMR has two driving wheels for flatform motion, and those are positioned on an axis passed through the WMR geometric center,

(6) Two passive wheel which have zero constraint are installed in front and rear of the flatform at the bottom for balance of WMR. So their motion can be ignored in the kinematic and dynamic models.

A welding torch is located to coincide the axis through the center of the two driving wheels. The radius of welding curve is sufficiently larger than turning radius of the WMR.
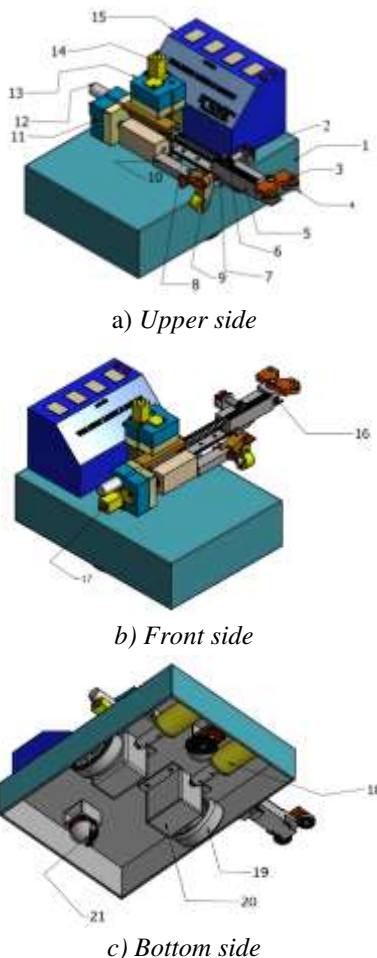

a) *Upper side*

b) *Front side*

c) *Bottom side*
Fig. 1: 3D configuration of the welding mobile robot
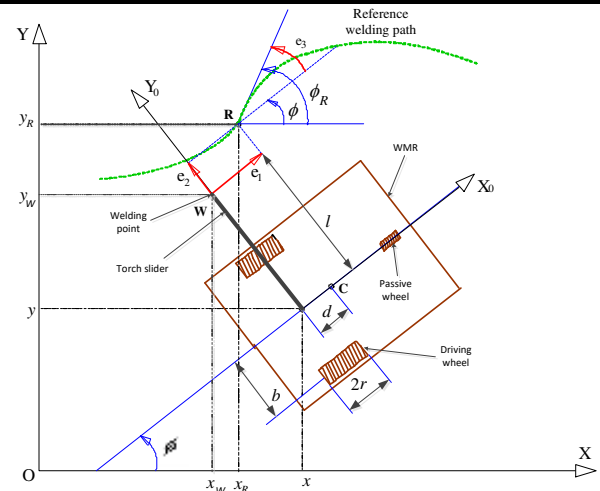

Fig. 2: Configuration for geometric model of the WMR in the Cartesian coordinates

The detailed componets of the welding mobile robot are presented in Table 1.

Table.1: Detailed coponents of the welding mobile robot

No.	Name	No.	Name
1	Platform	11, 20	Gear box
2	Potentiometer	12	Encoder
3	Rotary claw	13	Gear
4	Roller	14	DC motor acting on height of welding torch
5	Strainght gear	15	Display and keypad
6	Gear and bar	16	Potentiometer
7	Sliding bar	17	DC motor for controlling torch slider
8	Springs	18	DC motors acting on left and right wheels
9	Clamp mechanism	19	Left and right driving wheels
10	Welding hand grip	21	Passive wheel

2. DC Servo Motor Modeling

This section presents the modelingof DC servo motor [9]. Schematic of the the DC servo motor plus wheel is shown in Fig. 3.
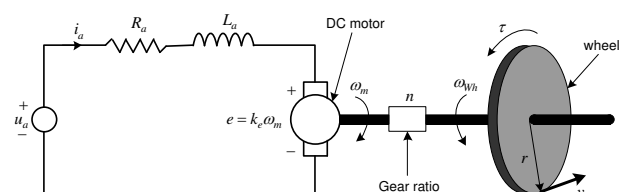

Fig. 3: Circuit schematic of the DC motor plus wheel

The dynamics of each DC servo motor is described as follows:

$$u_a = R_a i_a + L_a \frac{di_a}{dt} + k_e \omega_m \qquad (1)$$

Since the electrical time constant of the DC servo motor is very small compared to the mechanical time constant, the motor electric circuit dynamics can be neglected, which leads to $L_a \frac{di_a}{dt} = 0$.

Eq. (1) is rewritten as

$$i_a = (u_a - k_e \omega_m) / R_a \qquad (2)$$

The relation between ω_m and ω_{Wh} is

$$\omega_m = n\omega_{Wh} \qquad (3)$$

Torque of DC servo motor is given by

$$\tau = k_t i_a \qquad (4)$$

Substituting Eqs. (2)~ (3) into Eq. (4), the following is obtained

$$\begin{aligned} \tau &= k_t (u_a - k_e \omega_{Wh} n) / R_a \\ &= (k_t / R_a)u_a - (k_t k_e / R_a)\omega_{Wh} n \\ &= \alpha u_a - \beta \omega_W \end{aligned} \qquad (5)$$

where $\alpha = k_t / R_a$ and $\beta = k_t k_e n / R_a$ are motor characteristic coefficients depending on the parameters of DC servo motor.

3. Kinematic Modeling

A reference point R moving with the constant velocity of v_R, the coordinates (x_R, y_R) and the heading angle ϕ_R on the reference welding path satisfies the following equations:

$$\begin{cases} \dot{x}_R = v_R \cos\phi_R \\ \dot{y}_R = v_R \sin\phi_R \\ \dot{\phi}_R = \omega_R \end{cases} \qquad (6)$$

The kinematic equations for the center point of the WMR are set up as the following:

$$\begin{bmatrix} \dot{x} \\ \dot{y} \\ \dot{\phi} \end{bmatrix} = \begin{bmatrix} \cos\phi & 0 \\ \sin\phi & 0 \\ 0 & 1 \end{bmatrix} \begin{bmatrix} v \\ \omega \end{bmatrix} \qquad (7)$$

where $q = [x, y, \phi]^T$ is the posture vector of WMR rotating center point $C(x, y)$ in the Cartesian frame, $z = [v \quad \omega]^T$ is the actual velocity vector.

The relationship between v, ω and the angular velocities of right wheel ω_{rw} and left wheel ω_{lw} is given by

$$\begin{bmatrix} \omega_{rw} \\ \omega_{lw} \end{bmatrix} = \begin{bmatrix} 1/r & b/r \\ 1/r & -b/r \end{bmatrix} \begin{bmatrix} v \\ \omega \end{bmatrix} \qquad (8)$$

In Fig. 2, the kinematic equation of the welding point $W(x_w, y_w)$ which is fixed on the torch holder can be calculated from the WMR's center $C(x, y)$ as follows:

$$\begin{cases} x_w = x - l\sin\phi \\ y_w = y + l\cos\phi \\ \phi_w = \phi \end{cases} \qquad (9)$$

The derivative of Eq. (9) yields

$$\begin{bmatrix} \dot{x}_w \\ \dot{y}_w \\ \dot{\varphi}_w \end{bmatrix} = \begin{bmatrix} \cos\varphi & -l\cos\varphi \\ \sin\varphi & -l\sin\varphi \\ 0 & 1 \end{bmatrix} \begin{bmatrix} v \\ \omega \end{bmatrix} \qquad (10)$$

where l is assumed to be constant.

4. Developed Dynamic Modeling

In Fig. 2, using the references from [10] to [14], the developed dynamic equations of the WMR considering at DC Servo motor voltage level is rewrited as follows:

$$\overline{H}(q)\dot{z} + [\overline{B}(q,\dot{q}) + F]z + u_d = u \qquad (11)$$

where

$$\overline{H} = \frac{1}{\alpha} \begin{bmatrix} \frac{r^2}{4b^2}(mb^2 + I) + I_w & \frac{r^2}{4b^2}(mb^2 - I) \\ \frac{r^2}{4b^2}(mb^2 - I) & \frac{r^2}{4b^2}(mb^2 + I) + I_w \end{bmatrix},$$

$$\overline{B} = \frac{1}{\alpha} \begin{bmatrix} 0 & \frac{r^2}{2b}m_c d\dot{\phi} \\ -\frac{r^2}{2b}m_c d\dot{\phi} & 0 \end{bmatrix}, \quad F = \frac{\beta}{\alpha} \begin{bmatrix} 1/r & b/r \\ 1/r & -b/r \end{bmatrix},$$

$u_d = \overline{M}(q)f$, $u = [u_r \quad u_l]^T$, $m = m_c + 2m_w$,
$I = m_c d^2 + 2m_w b^2 + I_c + 2I_m$, $z = [v \quad \omega]^T$, $z_d = [v_d \quad \omega_d]^T$
, $f = [f_1 \quad f_2]^T$ $\qquad (12)$

III. INTEGRAL SLIDING MODE CONTROLLER DESIGN BASED ON DEVELOPED DYNAMIC MODELING FOR WELDING MOBILE ROBOT

Problem Statement: The objective is to design a nonlinear controller so that the welding point $W(x_w, y_w, \phi_w)$ tracks to the reference point $R(x_R, y_R, \phi_R)$ moving on a desired welding path at a constant velocity v_R.

In Fig. 2, the tracking error vector $e = [e_1, e_2, e_3]^T$ is defined as the difference between the welding point W and the reference point R as follows:

$$e = \begin{bmatrix} e_1 \\ e_2 \\ e_3 \end{bmatrix} = \begin{bmatrix} \cos\phi & \sin\phi & 0 \\ -\sin\phi & \cos\phi & 0 \\ 0 & 0 & 1 \end{bmatrix} \begin{bmatrix} x_R - x_W \\ y_R - y_W \\ \phi_R - \phi_W \end{bmatrix} \qquad (13)$$

Because torch length l is controllable based on the torch slider. The first derivative of e yields

$$\dot{e} = \begin{bmatrix} \dot{e}_1 \\ \dot{e}_2 \\ \dot{e}_3 \end{bmatrix} = \begin{bmatrix} -1 & e_2+l \\ 0 & -e_1 \\ 0 & -1 \end{bmatrix} \begin{bmatrix} v \\ \omega \end{bmatrix} + \begin{bmatrix} v_R \cos e_3 \\ v_R \sin e_3 - \dot{l} \\ \omega_R \end{bmatrix} \quad (14)$$

First, the kinematic controller is designed as follows

$$z_d = \begin{bmatrix} v_d \\ \omega_d \end{bmatrix} = \begin{bmatrix} l(\omega_R + C_3 e_3) + v_R \cos e_3 + C_1 e_1 \\ \omega_R + C_3 e_3 \end{bmatrix} \quad (15)$$

and the length of torch satisfies

$$\dot{l} = v_R \sin e_3 + C_2 e_2 \quad (16)$$

where $z_d \in R^{2\times 1}$ is a control velocity vector and C_1, C_2, C_3 is a positive values.

Second, the developed dynamic controller with voltage control input vector for DC servo motors is designed as follows:

$$u = \overline{H}(q)\dot{z}_d + [\overline{B}(q,\dot{q}) + F]z + \overline{H}(q)\mu \quad (17)$$

The velocity error vector e_v is defined as

$$e_v = z_d - z = [e_{v1} \quad e_{v2}]^T \in \Re^{2\times 1} \quad (18)$$

The sliding surface vector s_v is defined as

$$S_v = e_v + K_v \int e_v dt \quad (19)$$

Where K_v is a positive diagonal matrix and $S_v = [S_{v1} \quad S_{v2}]^T$ is an integral sliding surface vector.

Third, the auxilary control law $\mu = [\mu_1 \quad \mu_2]^T$ is designed as follows

$$\mu = QS_v + Psign(S_v) + K_v e_v \quad (20)$$

where

$$S_v = \begin{bmatrix} S_{v1} \\ S_{v2} \end{bmatrix}; Q = \begin{bmatrix} Q_1 & 0 \\ 0 & Q_2 \end{bmatrix}; P = \begin{bmatrix} P_1 & 0 \\ 0 & P_2 \end{bmatrix}; \quad f = \begin{bmatrix} f_1 \\ f_2 \end{bmatrix} \le \begin{bmatrix} f_1^m \\ f_2^m \end{bmatrix}.$$

Q_i and P_i, $i = 1,2$ are constant positive values. f_i^m, $i = 1,2$ is the upper bounded value of f_i

Theorem: For the kinematic modeling Eq. (10) and the developed dynamic modeling Eq. (11) of the welding mobile robot (WMR), if the control laws in Eqs. (15) and (17), Eq. (20) are applied, the tracking error vector e converges to zero asymtotically as $t \to \infty$.

Proof:
The Lyapunov function candidate is defined as follows:

$$V = V_1 + V_2 \ge 0 \quad (21)$$

where the conponents of the V function are chosen as:

$$V_1 = \frac{1}{2}(e_1^2 + e_2^2 + e_3^2) \ge 0 \quad (22)$$

$$V_2 = \frac{1}{2}S^T S \ge 0 \quad (23)$$

With the velocity control input Eq. (15), the $\dot{V}_1$ becomes

$$\dot{V}_1 = -C_1 e_1^2 - C_2 e_2^2 - C_3 e_3^2 \le 0 \quad (24)$$

The derivative of S_v in Eq. (19) is as the following

$$\dot{S}_v = \dot{e}_v + K_v e_v = (\dot{z}_d - \dot{z}) + K_v e_v \quad (25)$$

In other hand, from Eqs. (11) and (17), the following is obtained.

$$\dot{z}_d - \dot{z} = f - \mu \quad (26)$$

Substituting Eq. (26) into Eq. (25), Eq. (25) becomes as

$$\dot{S}_v = f - \mu + K_v e_v \quad (27)$$

With the control law Eq. (20), Eq. (27) becomes

$$\dot{S}_v = -QS_v - Psign(S_v) + f \quad (28)$$

Substituting Eq. (28) into the first derivative of V_2 in Eq. (23) is obtained.

$$\dot{V}_2 = S_v^T \dot{S}_v \le -S_v^T QS_v - |S_{v1}|(P_1 - f_1^m) - |S_{v2}|(P_2 - f_2^m) \quad (29)$$

If $Q_i \ge 0$ and $P_i \ge f_i^m$, $i = 1,2$ then $\dot{V}_2 \le 0$.

From Eqs. (21)-(23) and (24),(29), that is $\dot{V} \le 0$. By Barbalat's lemma [16] , $S_v \to 0$ as $t \to \infty$. Because there exists the control law μ stabilizing sliding surfaces go to zero, the velocity error vector $e_v \to 0$ and the control law z_d makes tracking error vector $e \to 0$. Because of both $e \to 0$ and $e_v \to 0$ that mean the welding point W of welding mobile robot tracks a reference point R which is moving on a desired welding trajectory at a constant velocity. Block diagram for the proposed nonlinear controller is shown in Fig. 4.
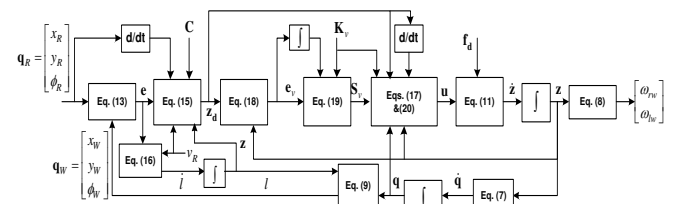

Fig.4: Block diagram for the proposed nolinear controller

IV.   ERROR MESUREMENT AND HARDWARE

1. Mesurement of tracking error using tourch sensor

In order to measure the tracking errors, a mechanical measurement scheme using potentiometers is shown in Fig. 5 [9]. Two rollers are placed at points O_2 and O_3. Two sensors for measuring the errors are needed. That is, they are one linear potentiometer sensor for measuring *ds* and one rotating potentiometer sensor for measuring the angle between the torch and the tangent line of the wall at the welding point.
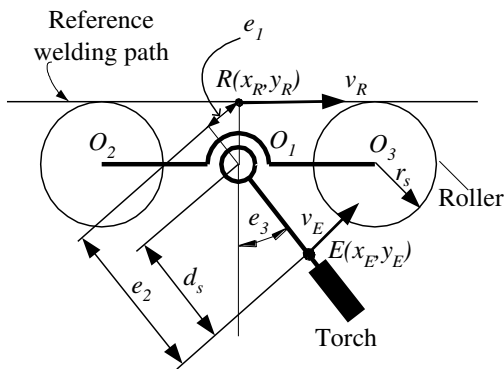
Fig. 5: Tracking errors measurement scheme

The tracking errors can be calculated as follows:

$$\begin{cases} e_1 = -r_s \sin e_3 \\ e_2 = (l_s - l) - r_s(1 - \cos e_3) \\ e_3 = \angle(O_1C, O_1O_2) - 90^0 \end{cases} \quad (30)$$

where O_2 and O_3 are the center points of roller O_2 and O_3 respectively, O_1 is the center point of O_2O_3, W is the point on torch holder, r_s is the radius of the roller, d_s is the length measured by the linear potentiometer, and e_3 is the angle measured by the rotating potentiometer. In Figure 5, the reference welding path is a line. When the reference welding path is a curve, Eq. (30) is also valid if the distance O_2O_3 is sufficiently small and the radius of the welding path is enough large.

2. Hardware of the system

Fig. 6 shows the control system configuration of welding mobile robot. The control system is based on the integration of microcontroller DSP F28335 and ATmega328. The microcontroller ATmega328 are used for two DC servo motor control signal of left wheel and right wheel and torch slider controller. The microcontroller DSP F28335 is used for main controller. The three servo controllers are controlled by main controller. The main controller functionalized as master links to the three servo controllers via I2C communication.
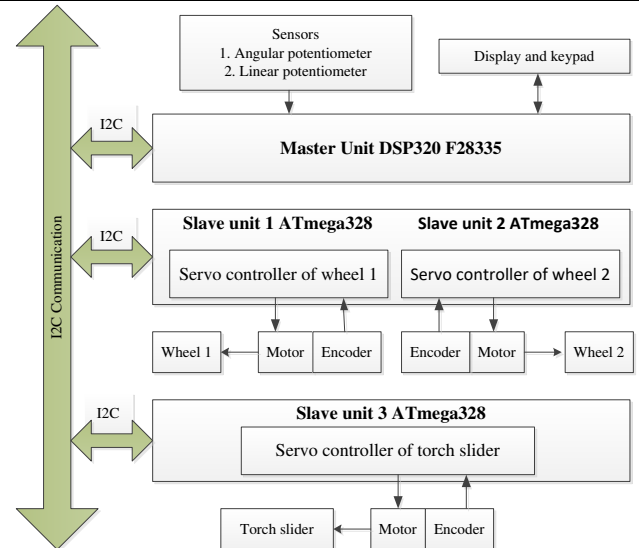

Fig. 6: Control system configuration of welding mobile robot

Fig. 7: Experimental welding mobile robot

The two A/D ports of the DSP F28355 are connected with the two potentiometers for sensing the tracking errors. The master unit send the commands to the slave controllers via I2C communication,respectively. The master unit can be used to interface other devices such as display and keypad devices for manual control. The sampling time of control system is 10ms. The slave unit integrates ATmega328 with motor drivers for the DC servo motor control. This slave controller can perform a complete servo operation with a closed loop feedback control using an encoder for velocity control of two wheels and position of welding torch. The experimental welding mobile robot is shown in Fig. 7 and its dimensions are shown in Table 3.

V. SIMULATION AND EXPERIMENTAL RESULTS

Fig. 8 shows the reference welding trajectory that has sinusoidal form. The reference welding point R moves from the start point to the stop point with a constant velocity v_R.
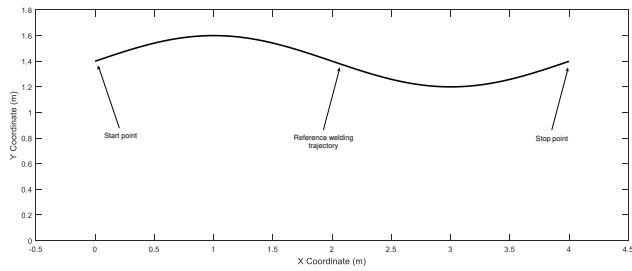
Fig. 8: The reference welding trajectory has sinusoidal
form $y = 0.2 sin(1.57x) + 1.4$

The designed parameters are as follows: $P_1 = 12.6 s^{-1}$, $P_2 = 15.3 s^{-1}$, $Q_1 = 22.5 s^{-1}$, $Q_2 = 26.4 s^{-1}$; and $C_1 = 16.3 s^{-1}$, $C_2 = 2.5 s^{-1}$ and $C_3 = 25.8 s^{-1}$, $K_{v1} = 0.3 s^{-1}$, $K_{v2} = 0.7 s^{-1}$, $f_{m1} = 0.5N$, $f_{m2} = 0.5N$. The numerical parameter values and the initial values for simulation are given in Tables 2-4.

Table 2. Numerical values of the DC servo motor's parameters

Parameters	Values	Units
R_a	20.5	[Ω]
k_e	7.2x10^{-2}	[Nm/A]
k_t	7.2x10^{-2}	[Nm/A]
u	24	[V]
τ	3.1	[kg.cm]
n	71	[rpm]

Table 3. The numerical parameters values for simulation and experimental

Parameters	Values	Units
b	0.12	[m]
r	0.03	[m]
d	0.015	[m]
m_c	12	[kg]
m_w	0.3	[kg]
I_c	0.32	[kgm^2]
I_w	0.024	[kgm^2]
I_m	3.6×10^{-4}	[kgm^2]
α	0.0035	[N.m/ V]
β	0.018	[Kg.m^2/ s]

Table 4. The initial values for simulation and experimental

Parameters	Values	Units
x_R	0	[m]
y_R	1.4	[m]
ϕ_R	25°	[deg]
x_W	0	[m]
y_W	1.38	[m]

ϕ	15°	[deg]
v_R	7.5	[mm/s]
v	0	[mm/s]
ω_R	0	[rad/s]
ω	0	[rad/s]
l	0.145	[m]

The simulation results for tracking welding path are shown in Figs. 9 to 17. Fig.s 9 and 10 show the movement of the WMR along the desired welding trajectory for the time beginning and full time 4000 seconds. The simulation results for error tracking vector during 5 seconds at beginning and 4000 secconds of full time are shown in Fig.s 11 and 12. The errors go to zero from 3 seconds. The linear velocity of welding point is shown in Fig. 13; its is shown that the linear velocity at the welding point w of the WMR has quick change at the first time and converges to the constant velocity in the vicinity of $7.5 mm/s$ as desired after 1 seccond.
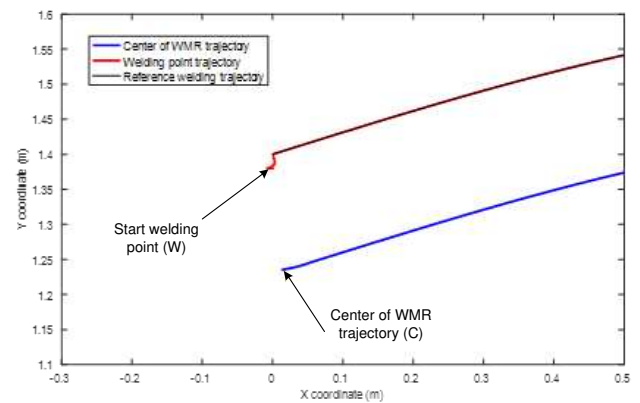

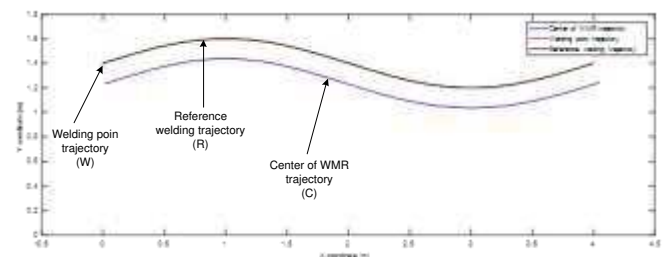*Fig. 9: Movement of the WMR at the beginning time*

Fig. 10: Movement of the WMR for full time (4000 seconds)
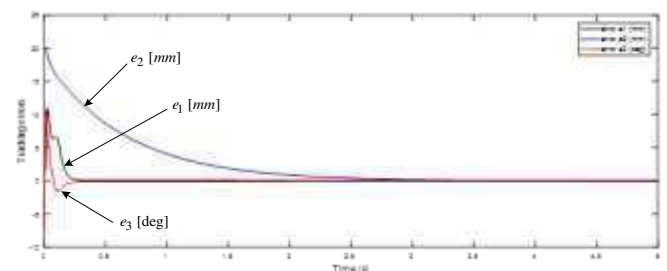

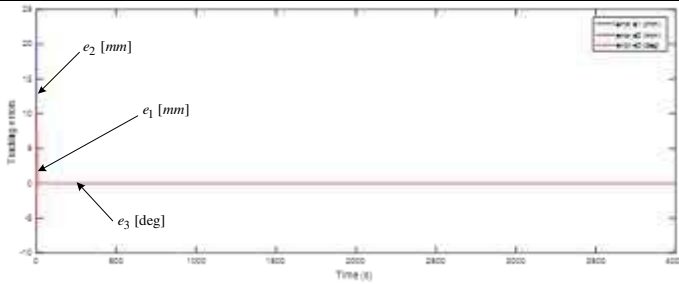*Fig. 11: Tracking errors at beginning time (5 seconds)*

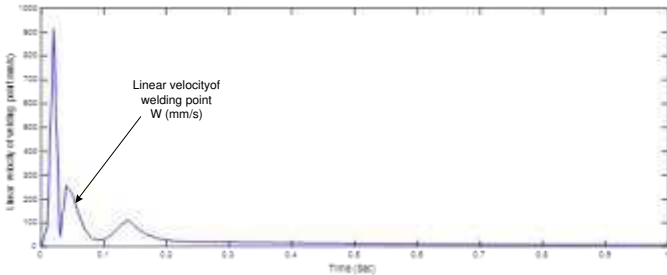*Fig. 12: Tracking errors for full time (4000 seconds)*

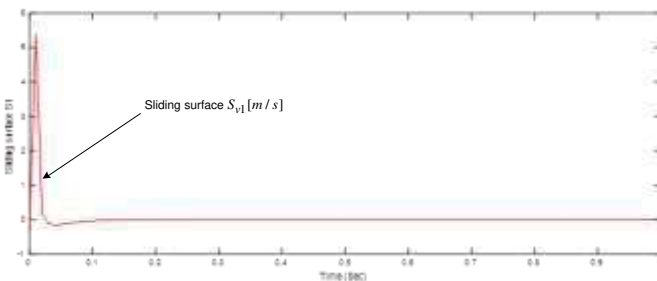*Fig. 13: Linear velocity of the welding point W*

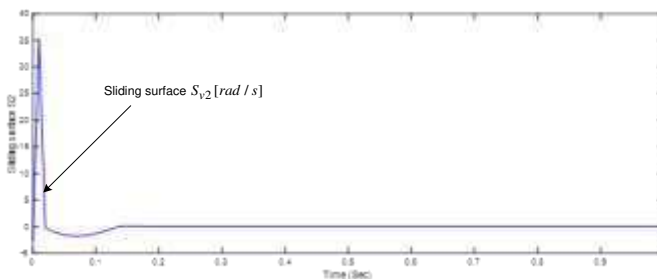
Fig. 14: Sliding surface S_{v1}

Fig. 15: Sliding surface S_{v2}

The sliding surfaces are shown in Figs. 14 to 15. They go to zero very quickly and keep zero value smoothly for full time. Fig. 16 shows the linear velocity and torch length of WMR. It goes from $145\,mm$ at initial time to $163.3\,mm$ after about 3 seconds and keeps the that value for remain time. Fig. 17 shows that the control input voltage vector u changes rapidly at the start time converges to small values from 0.3 second for the full time. Figs. 18 and 19 show the welding process of welding mobile robot and experimental welding line result respectively. The simulation and experimental results are shown that the WMR has good welding path tracking performance. It is so that the welding mobile robot can be applied in the practical welding industry field.
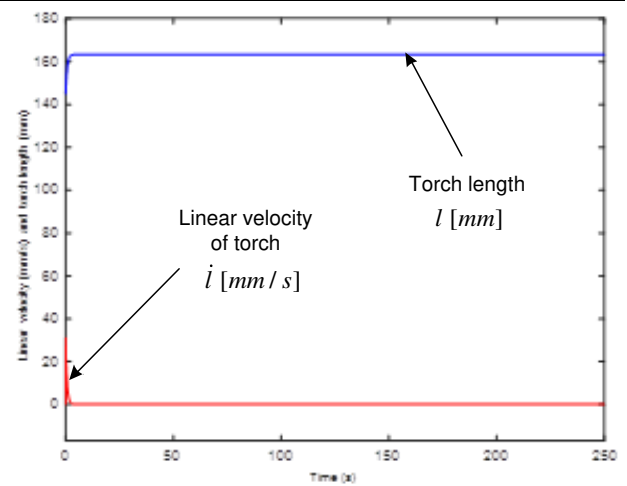

Fig. 16: Linear velocity ($\dot{l}$) and length (l) of welding torch at the beginning 250 seconds
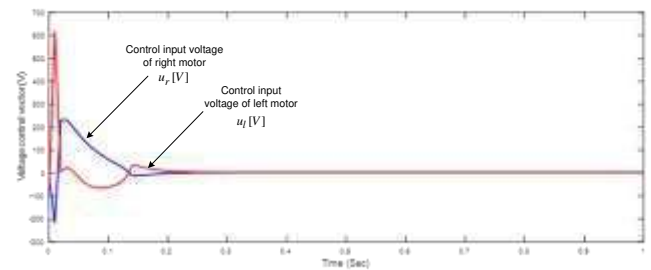

Fig. 17: Control input voltage vector at beginning time

Fig. 18: The experimental welding mobile robot

Fig. 19: Experimental welding line result

VI. CONCLUSION

This paper presents the proposed control scheme that makes the combination of a kinematic controller (KC) and an integral sliding mode dynamic controller (ISMC) based on the developed dynamic modeling for the welding mobile robot to track a desired welding trajectory at a desired velocity under external disturbances. The control laws are obtained by backstepping method. The system stability is proved based on Lyapunov theory. The control law stabilizes the sliding surface vector and makes the tracking error vector go to zero asymptotically. To implement the designed tracking controller, the control system is developed based on DSP F28355 and ATmega328. A scheme for measuring the posture tracking error vector using torch sensor is presented. The simulation and experiment results are shown to illustrate effectiveness and the applicability to the welding industry field of the proposed controller.

REFERENCES

[1] Y. H. John, W. Gao, C. H. James (1993). Variable Structure Control: A Survey. IEEE Transactions on Industrial Electronics (ISSN: 0278-0046), 40(1), 2-22.

[2] K. D. Young, V. I. Utkin, U. Ozguner (1999). A control engineer's guide to sliding mode control. IEEE Transactions on Control Systems Technology (ISSN: 1063-6536), 7(3), 328-342.

[3] Y. J. Huang, T. C. Kuo, S. H. IEEE Transactions on Control Systems Technology Chang. Adaptive Sliding Mode Control for Nonlinear Systems with Uncertain Parameters (2008). IEEE Transactions on Systems, Man, and Cybernetics (ISSN: 2168-2216), 38(2), 534-539.

[4] Y. Liu, Y. Li (2005). Sliding mode adaptive neural-network control for nonholonomic mobile modular manipulators. Journal of Intelligent and Robotic Systems (ISSN: 0921-0296(P) | 1573-0409(O)), 44(3), 203-224.

[5] S. Islam, X. P. Liu (2011). Robust Sliding Mode Control for Robot Manipulator. IEEE Transactions on Industrial Electronics (ISSN: 0278-0046), 58(6), 2444-2453.

[6] Y. Li, Y. Liu (2006). Real-time tip-over prevention and path following control for redundant nonholonomic mobile modular manipulators via fuzzy and neural-fuzzy approaches. Journal of Dynamic Systems, Measurement, and Control, Transactions of ASME (ISSN: 0022-0434(P) | 1528-90288(O)), 128(4), 753-764.

[7] H. Q. T. Ngo, J. H. Shin, W. H. Kim (2008). Fuzzy Sliding Mode Control for Robot Manipulator. Artificial Life and Robotics (ISSN: 1433-5298(P) | 2456-1908(O)), 13(1), 753-764.

[8] J. H. Lee, C. Lin, H. Lim, J. M. Lee (2009). Sliding Mode Control for Tracking Trajectory of Mobile Robot in The RFID Sensor Space. International Journal of Control, Automation, and System (ISSN : 1598-6446 (P) | 2005-4092 (O)), 13(1), 429-435.

[9] N. Hung, D. H. Kim, H. K. Kim, S. B. Kim. Tracking controller design of omnidirectional mobile manipulator system (2009). Proc. of ICROS-SICE International Joint Conference, Fukuoka International Congress Center (ISBN: 978-4-907764-33-3), 753-764.

[10] J. M. Yang, J. H. Kim (1999). Sliding mode control for trajectory tracking of nonholonomic wheeled mobile robots. IEEE Trans. on Robotics and Automation (ISSN: 1042-296X), 15(3), 578-587.

[11] N. Hung, Jae. S. I, S. K. Jeong, H. K. Kim, S. B. Kim (2010). Design of a Sliding Mode Controller for an Automatic Guided Vehicle and Its Implementation. International Journal of Control, Automation, and Systems (IJCAS) (ISSN: 1598-6446 (P) | 2005-4092 (O)), 8(1), 81-90.

[12] V. T. Dinh, N. Hung, S. M. Shin, H. K. Kim, S. B. Kim and G. S. Byun (2012). Tracking Control of Omnidirectional Mobile Platform with Disturbance Using Differential Sliding Mode Controller. International Journal of Precision Engineering And Manufacturing (ISSN: 2234-7593(P) | 2005-4602(O)), 13(1), 39-48.

[13] T. L. Chung, S. S. Park, T. H. Bui, S. B. Kim (2004). Sliding mode control of spot bead welding mobile robot. Proc. of KSPSE Conf. at MarineTime Univ., Korea, 229-236.

[14] T. L. Chung, T. H. Bui, T. T. Nguyen, S. B. Kim (2004). Sliding Mode Control of Two-Wheeled Welding Mobile Robot for Tracking Smooth Curved Welding Path. KSME International Journal (ISSN: 1738-494X(P) | 1976-3824(O)), 18(7), 1904-1106.

[15] N. Hung, Tuan. D. V, Jae. S. I, H. K. Kim, S. B. Kim (2010). Motion Control of Omnidirectional Mobile Platform for Trajectory Tracking Using Integral Sliding Mode Controller. International Journal of Control, Automation, and Systems (IJCAS) (ISSN : 1598-6446 (P) | 2005-4092 (O)), 8(6), 1221-1231.

[16] Jean-Jacques E. Slotine, Weiping Li (1991). Applied Nonlinear Control. Prentice-Hall International, Inc.